J. Chem. Soc., Faraday Trans. 2, 1989, **85**(8), 1003–1015

Stereochemical Influences in Atom–Triatomic Collisions

Zeyad T. Alwahabi, Carmel G. Harkin, Anthony J. McCaffery* and Benjamin J. Whitaker

School of Molecular Sciences, University of Sussex, Brighton BN1 9QJ

High-resolution dispersed fluorescence spectra from NH_2 in the electronically excited $\tilde{A}\ ^2A_1$ state have been obtained. Single quantum-state excitation using a tunable ring dye laser was employed and rotational energy transfer (RET) in the excited vibronic manifold was studied. Analysis shows that angular momentum based propensity rules are much more successful at predicting RET relaxation rates than are those based on the energy transfer. The results are interpreted with reference to the molecule-fixed axis system, and this allows us to work backwards to the incoming particle trajectory. Thus we obtain information about the stereochemistry of the NH_2 ($^2A_1$) + H interaction.

Collisionally induced transitions between the rotational levels of small molecules, particularly diatomics, have been extensively studied in recent years.[1,2] Of particular interest have been the attempts to formulate simple expressions for rates of rotational energy transfer (RET).[3–6] The motivations for this are in the ubiquitous nature of rotational relaxation in gas dynamics, and that an understanding of many important processes, for example cluster nucleation, requires the ability to calculate rotational relaxation rates quickly and efficiently. Full quantum-mechanical calculations are time-consuming and expensive, even for diatom–atom scattering, owing to the rapid computational explosion as the number of open rotational channels increases. Approximations, such as the infinite-order sudden (IOS), which decouple the scattering equations, have been very successful in predicting 'scaling' laws for RET.[7] More recently several semiempirical 'fitting' laws have been proposed,[3–6] and there has been considerable speculation as to their physical origin.[8] In particular it has been suggested that angular momentum constraints may be more important than energetic constraints.[9,10] In diatom–atom systems, however, this distinction is not clear cut since the transferred energy, $|\Delta E|$, scales as the transferred angular momentum, $|l|$, and thus the question is unresolved.

The study of atom–triatomic molecule collisions offers several interesting new possibilities which offset the obvious additional complexities in spectra and intermolecular potential. The most important of these is the existence of molecule fixed projections of the rotational angular momentum that are spectrally resolvable. In a bent triatomic or asymmetric-top molecule the rotational energy levels form stacks associated with the angular momentum, N, and its projection onto two of the molecular axes. Although the internal projections are not simultaneously rigorous quantum numbers, they do form a very valuable basis for spectroscopic identification and, more relevantly here, for visualising the molecular dynamics of scattering experiments.

Using high-resolution spectroscopic selection and detection techniques it is straightforward to isolate collisional processes which change the angular momentum vector and only one of the internal projection quantum numbers. In this way one is in effect sampling planar slices of the intermolecular potential. Thus experimentally one may isolate different aspects of the intermolecular potential by the simple device of fully spectroscopically resolving the initial and final states.

The particular system we have chosen to study is that of $NH_2 + H$. Aside from the intrinsic interest in NH_2 for the role it plays in atmospheric, interplanetary and combustion chemistry the radical is also an archetype of the Renner–Teller interaction. Thus NH_2 is unusual and spectroscopically complicated. Two particular points are important here. First, because NH_2 is a radical, the electronic states involved in the transitions of interest are both doublets and thus each rotational level is split through the effect of the spin–rotation interaction. An important consequence is that for open-shell collision partners we are faced with scattering on two distinct surfaces (singlet and triplet). Secondly, NH_2 is an asymmetric rotor, and consequently, as briefly discussed above, the rotational levels are split into a number $(2N+1)$ of sub-levels which depend on the relative orientation of the angular momentum vector to the molecule-fixed axis system. These states are usually labelled $N_{k_a k_c}$, where k_a and k_c refer to the projection of the angular momentum (excluding spin) onto the a and c axes of the molecule. We will see later that this will have important consequences when we consider rotational energy transfer between these levels.

The difficult and complex problem of collisional energy transfer of an open-shell molecule with an open-shell atom was first tackled by Shapiro and Kaplan[11] for the $OH + H$ system, and for the $NH_2 + H$ system by Dixon and Field.[12] In the latter paper rotational relaxation rates were interpreted in terms of the distorted-wave Born approximation which gave a semiquantitative fit to their experimental data.[13] Rotationally resolved fluorescence intensities were used to obtain relative rates of transfer from initially populated levels. Propensities such as $|\Delta N| \leqslant 2$ and $\Delta k_a = 0, 2$ (with $\Delta k_a = 0$ for $\Delta N = 2$) were observed for the $NH_2 + H_2/He$ system.† A correlation between the spin of the initially populated state and the collisionally populated state was observed for the *ortho* states, and consequently H atoms were thought by these authors to be the dominant collision partner. In contrast He atoms were thought to be responsible for collisional transfer between the *para* states. Subsequent time-resolved experiments[14] verified the $|\Delta N| \leqslant 2$ propensity rule and suggested that cascading (multiple collisions) might be responsible for the larger ΔN changes.

Somewhat earlier Kroll[15] had also observed energy transfer between the rotational levels in the $^2A_1$ state of NH_2. Although the collision partner was unspecified, Kroll found a significant retention of molecular orientation, in the laboratory-axis frame, after RET. A more systematic study at higher resolution of this polarisation transfer was later undertaken in our laboratory,[16,17] the results of which were interpreted in terms of an extended version of the perturbation treatment proposed by Dixon and Field.[12]

Experimental

The experimental arrangement is illustrated in fig. 1. NH_2 (amidogen) radicals were produced in a flow-reactor following the reaction of H atoms with hydrazine (N_2H_4). The reaction chamber consisted of a quartz discharge tube and a Pyrex flow-line equipped with gas inlet jets and observation/excitation ports fitted with fused silica windows. The observation cell was arranged so that laser-induced fluorescence could be detected either orthogonally to, or coaxially with, the excitation axis. The discharge tube and flow-line were etched with *ca.* 15% hydrofluoric acid for *ca.* 25 min prior to use in order to diminish radical destruction on the walls. The reactor was pumped by means of a double-stage rotary pump with a displacement of 80 $m^3 h^{-1}$ (Edwards model E2M 80). The H atoms were produced by microwave discharge at 2.45 GHz (Microtron model 200). In our initial experiments a gas mixture of H_2 in He (with a dilution of *ca.* 1:5) was used; however, in later experiments the H_2/He mix was replaced by water vapour, where it was found to produce more controllable experimental conditions and allowed

† NH_2 can be produced by the reaction of hydrazine with the products of a microwave discharge in H_2/He.

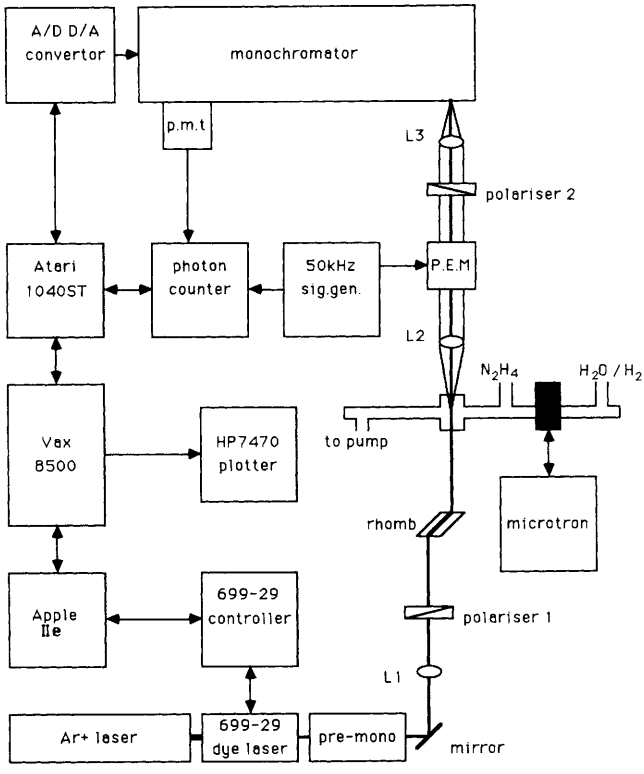

Fig. 1. The experimental set-up.

us to work at lower pressures. In both cases the total pressure in the flow line, as measured by a capacitance transducer downstream of the reaction zone (MKS Baratron model 222), was 1.5–2.0 Torr† for the H_2/He mix and *ca.* 0.6 Torr with water vapour. Hydrazine, 98% pure as supplied by Aldrich, was contained in a glass ampoule from where it was fed to the reactor inlet jet *via* PTFE tubing. The flow was controlled by a needle valve.

The reaction of H atoms with N_2H_4 results in hydrogen abstraction:

$$H + N_2H_4 \rightarrow H_2 + N_2H_3. \quad (1)$$

The NH_2 radicals are believed to be produced by subsequent reactions of the N_2H_3 radicals with H atoms.[18,19] A green flame is observed at the contact point which was found, on spectroscopic analysis, to be due to N_2^*, and probably arises from the recombination reaction of NH radicals. The NH radicals are in turn most probably the result of NH_2 recombination to yield NH and ammonia.

The output from a continuous-wave tunable dye laser (Coherent model 699-29) was directed so as to cross the flow tube *ca.* 10 cm downstream of the hydrazine inlet jet. The dye laser is controlled by a microcomputer (Apple IIe) which is connected to an integral wave-meter assembly. Thus it is possible to control the absolute wavelength of the laser to 4 parts in 10^7 (± 0.007 cm^{-1}). The spectral width of the dye laser (*ca.* 0.0003 cm^{-1}) was two orders of magnitude smaller than the Doppler width of NH_2 under our experimental conditions (0.054 cm^{-1} at 300 K). Transitions to the (0, 9, 0)

† 1 Torr = 101 325/760 Pa.

and (0, 10, 0) vibrational manifolds of the $\tilde{A}\,^2A_1$ first electronically excited state from the (0, 0, 0) manifold of the $\tilde{X}\,^2B_1$ ground state lie in the tuning range of rhodamine 6G. Excitations to individual rotation levels were assigned by monitoring the total laser-induced fluorescence using a photodiode attached to one of the optical windows of the observation cell, and scanning the frequency of the dye laser. Line positions were found to be in very good agreement with the published tables of Dressler and Ramsey.[20] The narrow linewidth of the laser allowed excitation into *each* spin component of any given rotational level, $J = N \pm 1/2$, in turn.

Once a transition had been assigned, the fluorescent light was collected by a lens and dispersed through a $\frac{3}{4}$ m double-grating Czerny-Turner monochromator (Spex model 1402). The gratings of this instrument were replaced with ones of 1800 grooves mm^{-1} giving a dispersion of 4 Å mm^{-1}. The dispersed fluorescence fell onto a Peltier cooled photomultiplier tube (EMI 9863B/100: S20 spectral response) and was detected by photon counting electronics (Brookdeal model 5C1). The photon counter and monochromator were interfaced to a micro-computer (Atari model 1040ST) which collected and stored the dispersed spectrum.

Two different experimental geometries were used in this study. In order to detect the degree of circular polarisation, $C = (I_+ - I_-)/(I_+ + I_-)$, the fluorescence was measured coaxially to the laser-beam propagation axis. In this case the output from the dye laser was first directed through a prism monochromator (Anaspec model 300S) to remove any background dye laser fluorescence before being passed through a linear polariser and then a Fresnel rhomb. The resultant circularly polarised light was then focused into the flow-reactor through one of the optical windows. The resultant fluorescence was collimated with an f 1.5 lens and passed through a photoelastic modulator (Morvue model PEMSF4) driven at 50 kHz and an analysing polariser before being focused onto the entrance slits of the monochromator. Further details can be found elsewhere;[21] however, the net result of this arrangement is to produce a modulated signal at the detector such that in one arm of the modulation cycle the signal is proportional to I_+, while in the other it is proportional to I_-. The photon counter can be operated in synchronous sampling mode so that these two signals could be recorded separately and the sum and difference easily computed and displayed.

In the second experimental arrangement the degree of linearly polarised fluorescence, $P = (I_\parallel - I_\perp)/(I_\parallel + I_\perp)$, could be obtained. In these experiments the Fresnel rhomb and premonochromator were removed from the optical train, and the fluorescence was collected orthogonally to the excitation axis. The driving frequency of the PEM was also changed to provide full-wave polarisation modulation. An additional advantage of this optical arrangement was that it was possible to observe the resonance fluorescence.

One final experimental consideration is that as a free radical the molecular g factor is quite large and Hanle depolarisation of the fluorescent light by magnetic fields is observable for modest field strengths (*ca.* 0.5 mT).[22] In order to guard against these effects a set of three pairs of Helmholtz coils (average diameter 30 cm) were constructed around the observation cell. The field at the centre of the coils was measured with a magnetometer (Schonstedt Instruments model DRM1) and nulled to $\pm 1\ \mu$T by varying the current in each pair of coils independently. In point of fact, for our particular laboratory orientation, the effects of the earth's magnetic field on the polarisation of the laser-induced emission appear to be negligible.[23]

Results

We have studied rotational energy transfer between a large number of states in the (0, 9, 0) and (0, 10, 0) vibrational manifolds of the $\tilde{A}\,^2A_1$ state of NH_2 and NHD. Here we wish to present results for excitation into the (0, 9, 0) Σ stack (*i.e.* states with $k_a = 0$), where we have made a systematic study of the relative rates of population, orientation

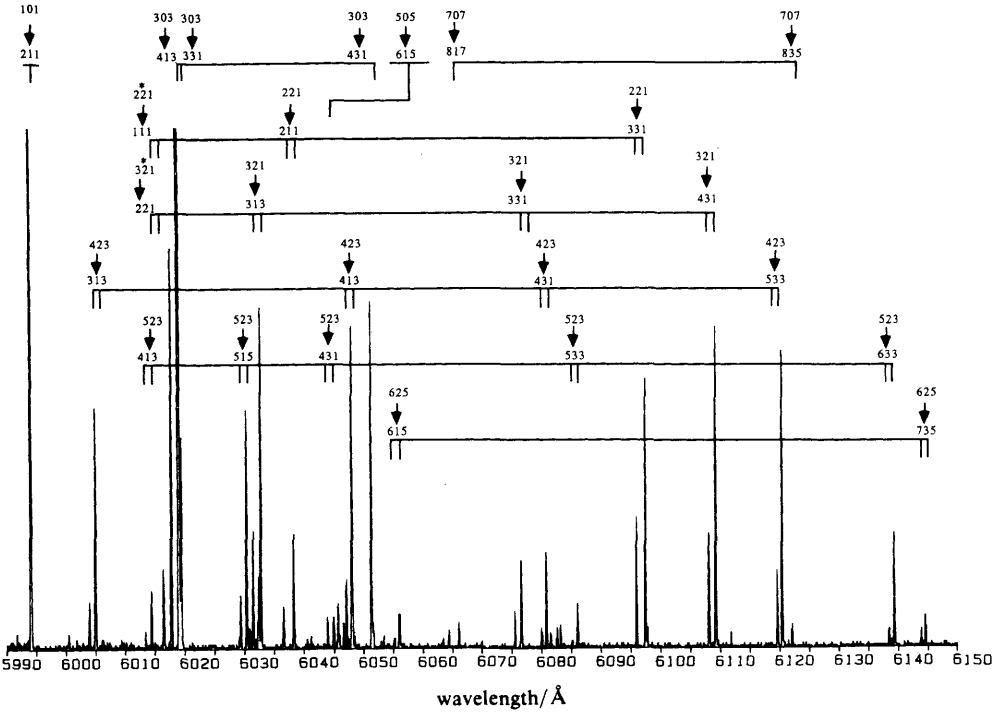

Fig. 2. Typical spectrum showing the dispersed fluorescence following excitation of the $(^2A_1)(0, 9, 0)3_{03}(J = 3.5)$ level from $(^2B_1)(0, 0, 0)3_{13}$.

and alignment transfer as functions of initially excited quantum number (including electron spin), and nuclear-spin symmetry. A typical dispersed fluorescence spectrum is shown in fig. 2. The signal-to-noise ratio on some of the resonance lines is greater than 3000:1. In general line strengths for excitation into the *ortho* levels are three times stronger than for the *para* levels because of the nuclear-spin statistics. As can be seen from the spectrum the spin-splitting in the Δ levels (*i.e.* $k_a = 2$) is well resolved, while for fluorescence from the Σ states, where the splitting is *ca.* 0.2 cm^{-1}, typically only a single line is visible owing the limited instrument resolution (*ca.* 0.3 cm^{-1}).

The results for population transfer are presented in tables 1–3. The tabulated results are divided into two sets according to whether the rotational transfer is to a state in the same k_a stack or crosses stacks. For each initial level $N_{k_a k_c}$ two sets of data are presented according to the initially excited spin component (except for the case of excitation into the 0_{00} level, where there is only one spin level). In order to obtain relative transfer rates from the fluorescence spectra the spectral line intensities must be taken into account. The computer program ASYMROT of Birss and Ramsey[25] was used to calculate the transition strengths, from which we deduced the relative populations of the collisionally excited levels.

The concurrent use of polarised light allows us to select simultaneously both space- and molecule-fixed axes. This comes about because polarised light will selectively excite the (degenerate) magnetic sub-levels of the selected rotational state, creating a distribution which for single-photon excitation is completely described by its first three Legendre moments. The state multipole moments are known as population, orientation and alignment. Experiments with circularly polarised light are mainly sensitive to the orientation, while linearly polarised light predominately probes the alignment. The

Table 1. Relative populations for intra Σ stack and inter Σ → Δ rotational energy transfer following P excitation of the 0_{00} level of the $^2A_1$ state

excitation $0_{00} \leftarrow 1_{10}$	radiative transition $^2A_1$-$^2B_1$	$\lvert l\rvert/\hbar$	$\Delta E/\mathrm{cm}^{-1}$	relative population $J_{ex} = 0.5$
Σ stack	0_{00}-1_{10}	0.00	0.00	1.000
	2_{02}-3_{12}	2.45	54.26	0.137
	4_{04}-5_{14}	4.47	181.78	0.018
Δ stack	2_{20}-1_{10}	2.45	−99.75	0.130
			−104.25	0.050
	3_{22}-2_{12}	3.46	−43.03	0.030
			−46.33	0.020
	4_{22}-3_{12}	4.47	30.36	0.025
			27.41	0.020

The relative populations of the collisionally populated states have been deduced from the line strengths of the observed transitions. Fitting these data against $|l|$ using eqn (3) gives: $a = 0.97$, $b = -0.97$, $R = -0.97$. The exponential-gap law,[24] $k_{N_{k_a k_c} \rightarrow N'_{k'_a k'_c}} = a \exp(-b|\Delta E|)$, gives: $a = 0.14$, $b = -0.011$, $R = -0.43$, where a and b are the free parameters and R is the correlation coefficient.

Table 2. As for table 1, but for Q excitation of 1_{01}

excitation $1_{01} \leftarrow 1_{11}$	radiative transition $^2A_1$-$^2B_1$	$\lvert l\rvert/\hbar$	$\Delta E/\mathrm{cm}^{-1}$	relative population $J_{ex} = 0.5$	relative population $J_{ex} = 1.5$
Σ stack	1_{01}-2_{11}	0.00	0.00	1.000	1.000
	3_{03}-4_{13}	2.13	90.75	0.084	0.080
Δ stack	2_{21}-3_{31}	2.00	−117.52	0.070	0.060
			−122.12	0.100	0.106
	3_{21}-4_{31}	2.60	−62.24	0.036	0.025
			−65.71	0.049	0.057
	4_{23}-5_{33}	3.27	13.79	0.011	0.015
			11.05	0.016	0.023
	5_{23}-6_{33}	4.21	106.17	0.009	0.005
			103.34	0.007	0.007

Fitting these data against $|l|$ using eqn (3) gives for $J_{ex} = 1.5$: $a = 1.01$, $b = -1.15$, $R = -0.99$, and for $J_{ex} = 0.5$: $a = 1.03$, $b = -1.20$, $R = -0.99$. The exponential-gap law gives for $J_{ex} = 1.5$: $a = 0.16$, $b = -0.014$, $R = -0.42$, and for $J_{ex} = 0.5$: $a = 0.15$, $b = -0.016$, $R = -0.44$.

linear polarisation ratios for transfer out of the 2_{02} state are given in table 4. In table 5 we show the results for circular polarisation following transfer out of the 3_{03} level.

Discussion

The rotational energy levels in the (0, 9, 0) vibrational manifold of $^2A_1$ of NH_2 are shown schematically in fig. 3, in which the spin splittings have been much exaggerated, although the ordering of the states is correct. Now referring to fig. 3 it is apparent, for example, that the 5_{23} level lies close to the 3_{03} level, in fact the energy gap is only 14 cm^{-1}. If energetic considerations were dominant one would expect efficient energy transfer on

Table 3. As for table 1, but for Q excitation of 3_{03}

excitation $3_{03} \leftarrow 3_{13}$	radiative transition $^2A_1$-$^2B_1$	$\lvert l\rvert/\hbar$	$\Delta E/\mathrm{cm}^{-1}$	relative population $J_{ex}=2.5$	relative population $J_{ex}=3.5$
Σ stack	1_{01}-2_{11}	2.13	−90.75	0.270	0.250
	3_{03}-4_{13}	0.00	0.00	1.000	1.000
	5_{05}-6_{15}	2.21	164.37	overlapped	0.140
	7_{07}-8_{17}	4.10	405.57	0.002	0.003
Δ stack	2_{21}-3_{31}	2.92	−208.27	0.040	0.070
			−212.87	0.080	0.060
	3_{21}-4_{31}	2.97	−152.99	0.030	0.090
			−156.46	0.080	0.070
	4_{23}-5_{33}	2.20	−76.96	0.019	0.072
			−79.70	0.065	0.042
	5_{23}-6_{33}	3.11	15.42	0.009	0.023
			12.59	0.020	0.010
	6_{25}-7_{35}	3.4	136.37	0.001	0.009
			133.92	0.005	0.010

Fitting these data against $|l|$ using eqn (3) gives for $J_{ex}=3.5$: $a=1.10$, $b=-1.13$, $R=-0.90$, and for $J_{ex}=2.5$: $a=1.16$, $b=-1.21$, $R=-0.92$. The exponential-gap law gives for $J_{ex}=3.5$: $a=0.13$, $b=-0.006$, $R=-0.35$, and for $J_{ex}=2.5$: $a=0.12$, $b=-0.007$, $R=-0.34$.

Table 4. *Linear polarisation ratios following Q excitation of* 2_{02}

excitation $2_{02} \leftarrow 2_{10}$	radiative transition $^2A_1$-$^2B_1$	$l/\hbar$	$\Delta E/\mathrm{cm}^{-1}$	linear polarisation $J_{ex}=1.5$	linear polarisation $J_{ex}=2.5$
Σ stack	0_{00}-1_{10}	2.45	−54.26	0.25 ± 0.09	1.78 ± 0.05
	2_{02}-2_{12}	0.00	0.00	18.67 ± 0.84	24.25 ± 2.8
Δ stack	2_{20}-2_{12}	2.83	−154.00	2.25 ± 2.1	2.47 ± 2.3
	3_{22}-3_{12}	2.08	−97.29	0.86 ± 0.05	4.51 ± 1.4
	3_{22}-3_{30}	2.08	−98.49	4.25 ± 2.8	6.95 ± 2.2
	4_{22}-4_{32}	2.86	−22.46	6.24 ± 1.9	11.12 ± 2.4
	4_{22}-4_{14}	2.86	−23.90	6.27 ± 0.5	3.75 ± 1.6

Note that the ratios here are given in %. Data are only presented for fluorescence from the same spin state as J_{ex}.

collision between these two states, since the cell temperature in our experiments, as determined from lineshape analysis, is 300 K. Examination of table 3, which presents the data for excitation into the 3_{03} spin doublets, shows that this is not the case. In fact the relative populations of the 5_{23} spin states are *ca.* a factor of four smaller than those of the 2_{21} states, which lie *ca.* 210 cm^{-1} from the laser-populated level. This is not simply an isolated example. Exponential-gap law[24] plots for all the population-transfer data presented in the tables show very poor linear correlation coefficients (see table captions), and clearly some other mechanism is at work.

Some insight is contained in the study by Orlikowski and Alexander of rotational energy transfer between the spin-orbit states of NO following collisions with Ar atoms.[26] As with NO, in NH_2 there are several stacks of rotational states within a given vibrational manifold; in the case of NO these are the two spin-orbit states separated by 123 cm^{-1},

Table 5. Circular polarisation ratios for R excitation of 3_{03}

excitation $3_{03} \leftarrow 2_{11}$	radiative transition $^2A_1$–$^2B_1$	$l/\hbar$	$\Delta E/\mathrm{cm}^{-1}$	circular polarisation $J_{ex} = 2.5$	circular polarisation $J_{ex} = 3.5$
Σ stack	1_{01}–1_{11}	2.13	−90.75	10.6 ± 2.50	15.2 ± 3.50
	1_{01}–2_{11}	2.13	−90.75	8.3 ± 2.00	11.6 ± 2.00
	3_{03}–3_{31}	0.00	0.00	16.6 ± 2.5	29.6 ± 4.0
	3_{03}–4_{13}	0.00	0.00	−13.1 ± 1.0	−10.4 ± 0.7
	3_{03}–3_{13}	0.00	0.00	16.8 ± 0.50	19.5 ± 0.50
Δ stack	2_{21}–1_{11}	2.92	−210.50	13.04 ± 2.0	23.6 ± 3.0
	2_{21}–2_{11}	2.92	−210.50	overlapped	20.6 ± 0.4
	3_{21}–3_{13}	2.97	−154.71	15.4 ± 0.2	13.5 ± 0.4
	4_{23}–4_{13}	2.20	−77.56	overlapped	15.2 ± 0.2
	4_{23}–3_{13}	2.20	−77.56	19.4 ± 2.5	24.2 ± 0.6

Ratios are given in %. Data are only presented for fluorescence from the same spin state as J_{ex}.

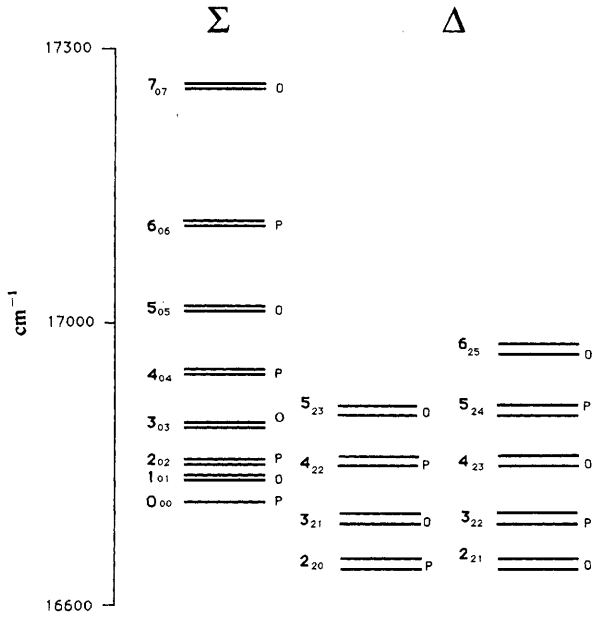

Fig. 3. Energy-level diagram for the Σ and Δ states of NH_2 in the (0, 9, 0) vibrational manifold of the $^2A_1$ state.

in NH_2 these are the Renner–Teller-coupled k_a states (Σ, Δ *etc.*). The authors were able to derive scaling laws for the intra- and inter-stack energy transfer in NO based on the properties of the angular momentum coupling coefficients which showed that for transfer between spin–orbit states, at least, vector-coupling considerations dominated energetic considerations.

For NH_2, as for any asymmetric rotor, the angular momentum vector of the nuclear frame can be projected onto any two of the molecular axes, and the magnitude of the angular momentum transferred on collision, $|l|$, will not scale simply with $|\Delta E|$ as it does in diatomic molecules. This is illustrated in fig. 4. The diagram illustrates the case

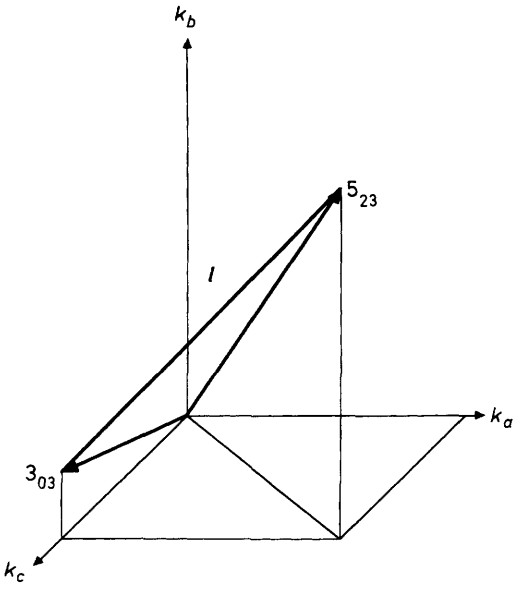

Fig. 4. The molecular-fixed projections of the 3_{03} and 5_{23} level. The vector $\boldsymbol{l}$ is the transferred angular momentum.

discussed above, that is collisional transfer from $3_{03} \rightarrow 5_{23}$. The collisionally transferred angular momentum can be obtained from geometrical considerations, and is given by:

$$l^2 = -2(N^2 + N - k_a^2 - k_c^2)^{1/2}(N'^2 + N' - k_a'^2 - k_c'^2)^{1/2} + N^2 + N - 2k_a k_a' - 2k_c k_c' + N'^2 + N'. \quad (2)$$

Since the energy-gap law gives a poor fit to rate constants for transferred population it is of interest to see how these scale with the transferred angular momentum, $|l|$. In contrast to the case for transferred energy, scaling with transferred angular momentum, according to an inverse exponential law,

$$k_{N_{k_a k_c} \rightarrow N'_{k'_a k'_c}} = a \exp(-b|l|) \quad (3)$$

is found to give an excellent fit to a wide range of data. The correlation coefficients for this law are given in the tables. All the data presented here can be accounted for with the parameters $a = 1.06 \pm 0.07$ and $b = 1.13 \pm 0.08$ with a reduced χ^2 of 0.3. However, an additional point needs to be made. In the analysis we have only considered data for like spin doublet components. That is if the state $J = N + \frac{1}{2}$ was excited we have tried only to fit data for transfer to the state $J' = N' + \frac{1}{2}$ and *vice versa* (for intra Σ stack transfer, where relative transfer rates of the spin components cannot be resolved, we have simply assumed that $\Delta M_S = 0$ makes the dominant contribution). When the electron spin is explicitly included the calculation of $|l|$ does not correctly predict the spin-branching transfer. This result can only be explained in terms of a spin-correlated interaction potential (*i.e.* an open-shell collision partner). The fact that the results are independent of the source H atoms indicates that hydrogen is the dominant collision partner in both *ortho* and *para* levels.

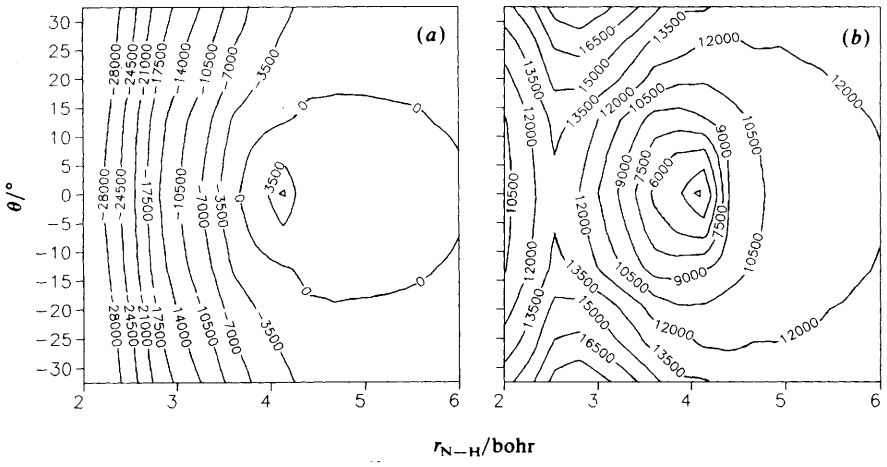

Fig. 5. The potential energy surfaces for the A (*a*) and X (*b*) states of ammonia. Contour levels are in cm^{-1} from the ground ($^2B_1$) state of NH_2 drawn from the data of ref. (28). The NH_2 fragment is taken to have a bond angle of 120° and a bond length of 2.0 bohr. The angle θ is relative to the plane containing the NH_2 group. The triangle marks the point of conical intersection between the two surfaces.

Using a hard-sphere approximation *ca.* 20 collisions would be expected during the radiative lifetime (*ca.* 10 μs)[27] of excited NH_2; in fact, rather more than this are likely to occur since the cross-section for rotational de-excitation will be somewhat larger than gas kinetic. It may therefore be argued that our experiment does not give nascent rotational distributions, but the result of cascading as suggested by Dearden *et al.*[14]

For a number of reasons we do not believe that we are observing multiple collisions. The first of these may be found by examining the NH_3 surface, illustrated in fig. 5. Recent calculations[28] are in very good agreement with experiment,[29] and the surface is believed to be very accurate. An important feature of the surface is the existence of a conical intersection for H atoms approaching along the *b* axis of ($^2A_1$) NH_2. The N—H distance at which the cusp occurs is highly dependent on the H—N—H bond angle. The situation illustrated in fig. 5 is for HNH = 120°. For linear NH_2 the $^2A_1$ and $^2B_1$ states are degenerate (correlating to a $^2\Pi$ state) and the conical intersection occurs at $r_{N-H} = \infty$. The vibrational period of the (0, 9, 0) states is estimated, assuming no anharmonicity, to be *ca.* 6 fs, which is two orders of magnitude smaller than the flight time of an H atom at 300 K through a 1 nm diameter interaction zone (400 fs), so that during the interaction the H atom will sample many different forms of the surface, and is highly likely to meet the cusp. The rapidly changing topology of the $NH_2 + H$ surface is an unusual situation (quite unlike the interaction potential of a vibrating diatomic and an atom). Classical trajectory studies by Dixon[30] show efficient quenching on the ($^2A_1$)NH_2 + H surface, so it is likely that the majority of collisions transfer molecules non-radiatively into ground-state species either reacting to form NH_3 or quenching to ($^2B_1$)NH_2. This would leave in the excited state just those molecules that have undergone essentially single-collision events.

Further evidence for this proposal comes from our polarisation data. The polarisation of the emitted light observed in the resonance lines is near to theoretical, and significant polarisation is observed in the transferred features (see tables 4 and 5). These observations are obviously inconsistent with a large number of collisions per excited state lifetime. Furthermore, the polarisation ratio appears to increase as the pressure in the cell increases.

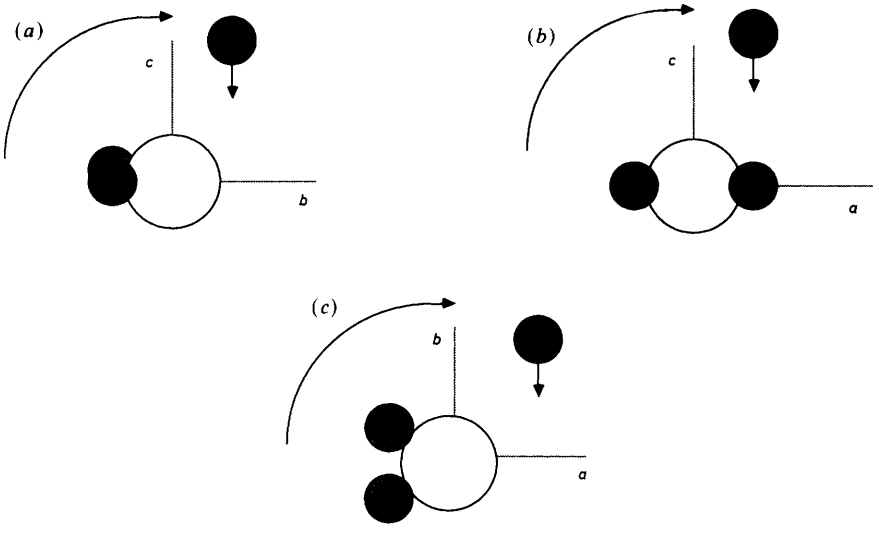

Fig. 6. The stereochemistry of the $(^2A_1)NH_2 + H$ system as probed by laser-induced fluorescence. (*a*) *N*, k_a-changing collisions (rotation in the *b*–*c* plane about the *a* axis). (*b*) *N*, k_a, k_c-changing collisions (rotation in the *a*–*c* plane about the *b* axis). (*c*) *N*, k_c-changing collisions (rotation in the *a*–*b* plane about the *c* axis).

What is unique about scattering studies of asymmetric rotors is the ability to back-project to the sub-set of trajectories, in the molecular frame, responsible for a particular transition. The correlation between $\boldsymbol{l}$ and the rotational relaxation rate is important because, being a vector quantity, the transferred angular momentum has direction as well as magnitude. Consequently in a collision between an H atom and an amidogen radical which results in RET with a given vector $\boldsymbol{l}$ a unique trajectory (or at least a sub-set of trajectories) can be ascribed to the incoming atom. Thus the experiment is capable of giving direct and accurate information on the fundamental stereochemistry of the interaction.

Molecules in the Σ stack are rotating about the *c* axis. Collisions with H atoms moving in the *a*–*b* plane will lead to intra-stack transfer, while collisions with atoms moving predominantly in the *b*–*c* plane will lead to inter-stack ($\Sigma \rightarrow \Delta$) transfer (see fig. 6). Unfortunately we do not know the topology of the surface for approach in the *b*–*c* plane. Some of our data, however, show that these latter collisions are more depolarising than those in the *a*–*b* plane, although not consistently so. The evidence from the population-transfer study indicates that there is essentially no difference between the rates of inter- and intra-stack transfer; however, there is some evidence to show that the spin-branching ratio is larger for inter-stack transfer, which we tentitively propose might be explained by the triplet surface lying closer to the singlet in the *b*–*c* plane. Further work is in progress, particularly with regard to the interpretation of the polarisation data.

Conclusions

Asymmetric-top molecules have a unique role to play in collision dynamics by virtue of the rotational levels possessing molecule-fixed projections of the angular momentum

vector. In cases where the quantum states are spectroscopically resolvable, laboratory-fixed axes may be unambiguously tied to those fixed on the molecule by optical excitation and then identified after collision by high-resolution spectroscopic detection.

A study of energy transfer in ($^2A_1$) NH_2+H collisions has been presented and a feature of this molecule is that full spectroscopic resolution of quantum levels, including spin, is feasible. A wide range of rotational energy-transfer results have been obtained and it is clear that by comparison with diatomics, the behaviour is anomalous with no apparent scaling relationship for rotational relaxation rates to transferred energy. However, the relationship with transferred angular momentum is very close and a momentum-gap law provides a quantitative fit to all our data. The key parameter in this law is the angular momentum transferred on collision. The magnitude and direction of $\boldsymbol{l}$ may be calculated from simple geometric considerations given values of N, k_a, and k_c for the initial and final states. Specific values of $\boldsymbol{l}$ can only arise from a limited set of H-atom trajectories and thus the possibility arises that sets of $N_{k_ak_c}$-resolved collision dynamic data may be used in conjunction with simple trajectory calculations to build up an intermolecular potential in at least two orthogonal planes, giving genuine stereochemical information.

Polarisation data augment this treatment and yield greater insight through the retention or loss of correlation by collision. Furthermore, spin-branching ratios are an indicator of the importance of the triplet surface. Both of these aspects of this problem will be addressed in forthcoming publications.

We are grateful to the S.E.R.C. for financial support, and for the award of a Research Studentship (C.G.H.) and an Advanced Research Fellowship (B.J.W.). The assistance of the Iraqi government is also gratefully acknowledged (Z.T.A.).

References

1 A. J. McCaffery, M. J. Proctor and B. J. Whitaker, *Annu. Rev. Phys. Chem.*, 1986, **37**, 223.
2 M. Faubel and J. P. Toennies, *Adv. At. Mol. Phys.*, 1977, **13**, 229.
3 T. A. Brunner and D. E. Pritchard, in *Dynamics of the Excited State*, ed. K. P. Lawley (John Wiley, Chichester, 1982).
4 C. Nyeland, *Chem. Phys. Lett.*, 1984, **109**, 603.
5 J. Derouard, *Chem. Phys.*, 1984, **84**, 181.
6 B. J. Whitaker and Ph. Bréchignac, *Laser. Chem.*, 1986, **6**, 61.
7 A. E. DePristo and H. Rabitz, *Chem. Phys.*, 1977, **24**, 2014.
8 N. Smith and D. E. Pritchard, *J. Chem. Phys.*, 1981, **74**, 3939.
9 B. J. Whitaker and Ph. Bréchignac, *Chem. Phys. Lett.*, 1983, **95**, 407.
10 M. A. Hoffbauer, S. Burdenski, C. F. Giese and W. R. Gentry, *J. Chem. Phys.*, 1983, **78**, 3832.
11 M. Shapiro and H. Kaplan, *J. Chem. Phys.*, 1979, **71**, 2182.
12 R. N. Dixon and D. Field, *Proc. R. Soc. (London), Ser. A*, 1979, **366**, 225.
13 R. N. Dixon and D. Field, *Proc. R. Soc. (London), Ser. A*, 1979, **366**, 247.
14 S. J. Dearden, R. N. Dixon and D. Field, *J. Chem. Soc., Faraday Trans. 2*, 1982, **78**, 1423.
15 M. Kroll, *J. Chem. Phys.*, 1975, **63**, 319.
16 B. J. Whitaker and A. J. McCaffery, *Chem. Phys. Lett.*, 1981, **86**, 185.
17 B. J. Whitaker and A. J. McCaffery, *J. Chem. Phys.*, 1983, **78**, 3857.
18 M. Gehring, K. Hoyerman, H. G. Wagner and J. Wolfrum, *J. Chem. Phys.*, 1971, **75**, 1287.
19 M. Arvis, C. Devillers, M. Gillois and M. Curtat, *J. Phys. Chem.*, 1974, **78**, 1356.
20 K. Dressler and D. A. Ramsey, *Philos. Trans. R. Soc. London, Ser. A*, 1959, **251**, 553.
21 R. A. Shatwell and A. J. McCaffery, *J. Phys. E*, 1974, **7**, 297.
22 M. Kroll, *J. Chem. Phys.*, 1975, **63**, 1803.
23 C. G. Harkin, A. J. McCaffery and B. J. Whitaker, unpublished results.
24 J. C. Polanyi and K. P. Woodall, *J. Chem. Phys.*, 1972, **56**, 1563.
25 F. W. Birss and D. A. Ramsey, *Comp. Phys. Commun.*, 1984, **38**, 83.
26 T. Orlikowski and M. H. Alexander, *J. Chem. Phys.*, 1983, **79**, 6006.
27 S. Mayama, S. Hiraoka and K. Obi, *J. Chem. Phys.*, 1984, **80**, 7.
28 M. I. McCarthy, P. Rosmus, H. J. Werner, P. Botchwina and V. Vaida, *J. Chem. Phys.*, 1987, **86**, 6693.

29 V. Vaida, M. I. McCarthy, P. C. Engelking, P. Rosmus, H. J. Werner and P. Botchwina, *J. Chem. Phys.*, 1987, **86**, 6669; M. N. R. Ashfold, C. L. Bennet, K. N. Rosser, R. J. Stickland and C. M. Western, *Chem. Phys.*, 1986, **101**, 467.
30 R. N. Dixon, personal communication.

Paper 8/03400A; *Received* 5*th August*, 1988